

## CARBON NANOWALLS DECORATED WITH GOLD NANOPARTICLES FOR SURFACE-ENHANCED RAMAN SPECTROSCOPY

S. MIHAI<sup>a</sup>, D. L. CURSARU<sup>a</sup>, D. MATEI<sup>a</sup>, A. DINESCU<sup>b</sup>, S. D. STOICA<sup>c</sup>,  
S. VIZIREANU<sup>c,\*</sup>, G. DINESCU<sup>c</sup>

<sup>a</sup>*Petroleum – Gas University of Ploiesti, Bucharest Av. 39, 100680, Ploiesti, Romania*

<sup>b</sup>*National Institute for Research and Development in Microtechnologies, Bucharest, Romania*

<sup>c</sup>*National Institute for Laser, Plasma and Radiation Physics, 409 Atomistilor Street, 77125 Magurele, Bucharest, Romania*

In this paper, we report a hybrid platform for the detection of low-concentration molecules by Surface-Enhanced Raman Spectroscopy (SERS). It is based on carbon nanowalls decorated with gold nanoparticles, and its sensitivity is demonstrated using Rhodamine B as analyte. With this substrate, it was possible to detect Rhodamine B, with concentrations lower than  $10^{-10}$  M. The detection limits is related to the large surface area of carbon nanowalls (CNW) with affinity for aromatic molecules, offering also accommodation to a large number of nanoparticles and to an enhanced coupling of the incident light to surface plasmons of gold nanoparticles. These results are relevant for development of optical sensing platforms based on SERS signals.

(Received April 20, 2018; Accepted August 15, 2018)

*Keywords:* SERS, Carbon nanowalls, Vertical graphene, Rhodamine B

### 1. Introduction

The current research focuses on developing methods for obtaining nanostructured materials with special functional properties. Surface-Enhanced Raman Spectroscopy (SERS) is a fast and reliable bio-detection procedure with the main advantage of simple sample preparation and operation compared to other methods [1]. The SERS technique has attracted attention over the years due to rapid detection of special materials in DNA sequencing [2,3] and pathogens [4], and having the ability of single molecule detection [5-9]. Therefore, this technique was widely extended to biomedical applications and biodetection [10] for various analytes in low concentrations.

SERS is a highly-effective tool based on the excitation of surface plasmon resonances that greatly enhance the Raman signal of molecules close to metal nanoparticles (especially Ag [11], Au, Cu [1,12-14] in the local electromagnetic field. The resonant excitation of surface plasmons in metallic nanostructures provides an opportunity to locate the light at nanoscale level, below to the light wavelength [15]. Strong localization of electromagnetic field in the vicinity of metallic nanostructures induce a nanofocusing effect, leading to enhancement of Raman scattering at the surface, phenomena known as SERS effect [16]. By decrease the spacing/gap in between nanoparticles, the nanofocusing effect is stronger and encounters so-called hot spot effect [17].

Graphene materials are versatile nanostructures [10] that can play a double role in the plasmonic optical sensors, both as receivers and transmitters. It is known that graphene has a high affinity for aromatic-ring containing biomolecules [18]. Wu et al. [19] demonstrated that Au-graphene sensors are more sensitive than usually SPR (Surface Plasmon Resonance) biosensors based on gold due to their better adsorption of benzene rings of biomolecules on graphene, thus leading to sensitivity increase up to 25%.

---

\*Corresponding author: s\_vizi@infim.ro

Vertical graphene can be used in combination with metal nanoparticles to form metal-graphene nanohybrid platforms for SERS [20,21]. Rider et al. [22] used vertical graphene substrates decorated with gold. Compared to horizontal graphene single layers (flat sensor area), better efficiency of gold nanoparticles distribution on graphene walls (bookshelf-like structures) with greater particle density (225%) was obtained by using vertical graphene layers. In this paper, we report on synthesis of carbon nanowalls (CNW) layers consisting from stacks of vertical oriented graphene (graphene oxide as found in XPS [23]) decorated with Au clusters, and their testing for detecting analyte molecules like Rhodamine B, at increased sensitivity.

We successfully detected Rhodamine B in concentrations as low as  $10^{-10}$  M by using these hybrid Au@CNW architectures as SERS platforms, a lower value compared with the platforms based on Ag@CNW, for which a detection limit of  $10^{-8}$  M [11] was reported.

## 2. Material and methods

### 2.1 Materials. Synthesis of the Au@CNW hybrid platform

The carbon nanowalls were prepared on silicon wafers (2x2 cm size) by a plasma jet generated in Ar/H<sub>2</sub>/C<sub>2</sub>H<sub>2</sub> gases at a flow rate of 1400/25/1 sccm, pressure p=130 Pa, RF power P<sub>rf</sub>=300 W and substrate temperature T=700 °C [24]. To prevent the agglomeration of nanoparticles on the CNW hydrophobic layers, the samples were treated by plasma jets Ar/N<sub>2</sub> (100/10 sccm) for 10 minutes to create a hydrophilic surface [23] and to create attachment centers for uniform decoration [25].

The Gold nanoparticles were prepared by the reaction of the Schiff base with tris (triphenylphosphinegold) oxoniumtetrafluoroborate at room temperature, as described elsewhere [26,27]. The necessary chemicals: ortho-vanillin, 4-aminoantipirine, acetonitrile, and ethanol were purchased from Sigma-Aldrich, whereas the (tripheylphosphinegold) oxoniumtetrafluoroborate was provided by Stem Chemicals.

The SERS hybrid substrate was obtained by chemical deposition of gold nanoparticles during immersion of carbon nanowalls in solution, resulting in Gold-supported CNW platforms. The analyte molecules were deposited onto these platforms by immersing them for two minutes in Rhodamine B solution and then dried in environmental conditions.

### 2.2. Material characterization and optical detection

The morphology of the hybrid platform (Au@CNW) was examined by scanning electron microscopy (SEM) using a (FESEM) Vega II LMU, and by atomic force microscopy (AFM) using a NT-MDT instrument.

The Raman spectra were recorded by a DXR Raman Microscope from Thermo Scientific, by using a 785 nm laser wavelength, with a laser power of 14 mW and an integration time of 12 s. The spot size was 0.25 microns. The presented spectra resulted from averaging onto various spots.

## 3. Results and discussions

The SERS effect can be achieved when an analyte molecule is adsorbed to a high-area solid substrate decorated with metallic nanoparticles or to metallic surfaces with nanoscale roughness. We selected carbon nanowalls (CNW) decorated with gold nanoparticles due to a high surface area, the inherent nano-micro topography, and the affinity of this graphene based material for aromatic molecules [17]. A schematic view Au@CNW platform is shown in Fig. 1.

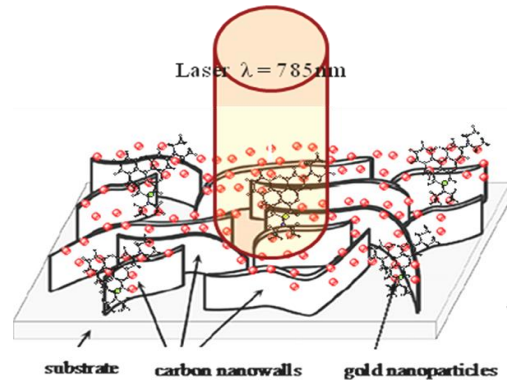


Fig. 1. Schematic illustration of the hybrid substrate

The Raman spectra of CNW and of Au-decorated CNW appear in Fig. 2 (black and red lines) as typical Raman spectra of vertical graphene structure [28]. Both spectra present similar bands (D, G bands and their second-order combination), similar position and the same bandwidth. A small increase in the D band for Au-decorated CNW can be noticed, but the spectrum reveals a conservation of vibrational structures of CNW platform after decoration with gold nanoparticles.

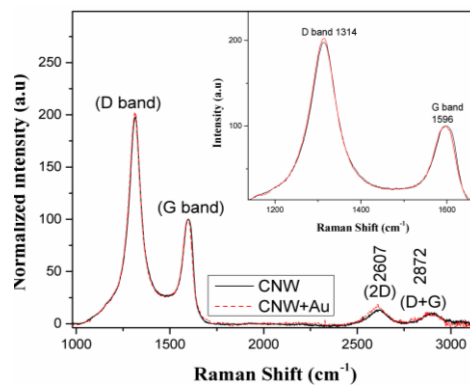


Fig.2. Raman spectra of CNW and gold nanoparticles decorated CNW

The main characteristic of the nanowalls template is the surface topography with a variety of surface features: sharp edges, rolls, hot spots, nanogaps, nanocavities [29]. For examination of the topography of the carbon nanowalls decorated with gold nanoparticles (Au@CNW), we performed atomic force microscopy (AFM) on a  $5 \times 5 \mu\text{m}^2$  area. The AFM results presented in Fig. 3 show a rough surface, with RMS (root-mean-square) surface roughness of about 61 nm, typical for CNW.

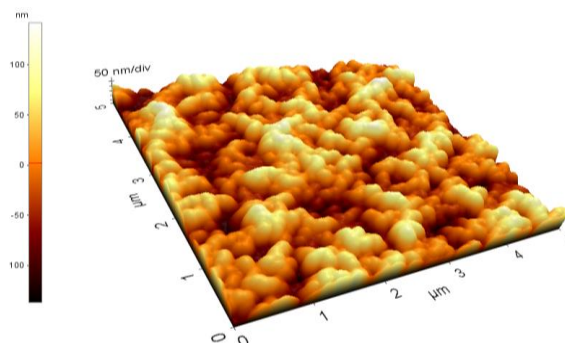


Fig. 3. AFM topographical image of hybrid platform (Au@CNW)

The actual morphology of the (Au@CNW) is best characterized by Field Emission Scanning Electron Microscopy (FE-SEM) and Transmission Electron Microscopy (TEM). Fig. 4 a, b) shows the SEM images of carbon nanowalls decorated with gold nanoparticles. It reveals the spreading of gold nanoparticles anchored on carbon nanowalls. The gold nanoparticles have size between of 5-8 nm onto inner CNW wall and occasionally some particles agglomerate in clusters of about 20 nm on CNW edges (see TEM image on Fig. 4 c, d).

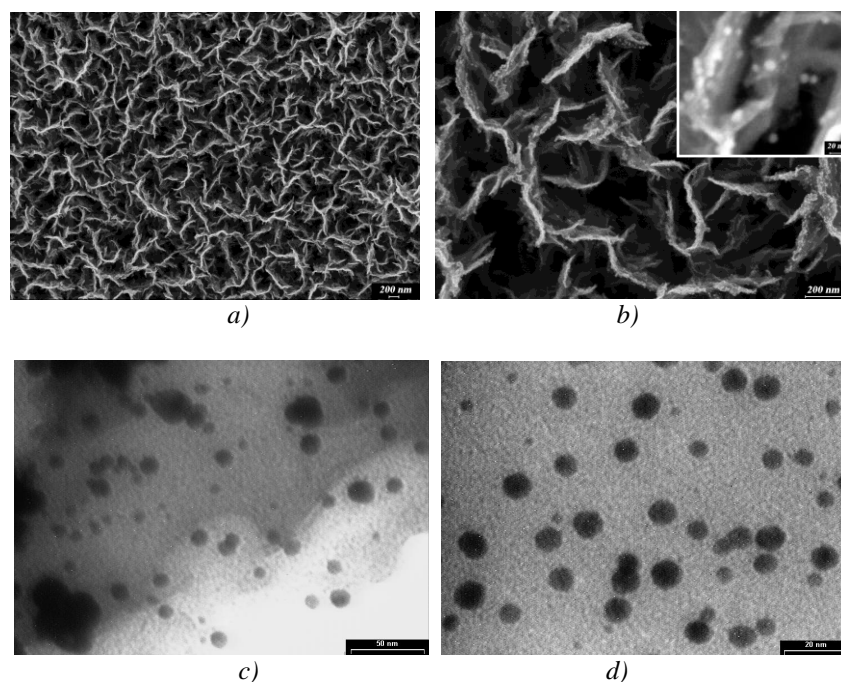


Fig. 4. FE-SEM images of CNW@Au hybrid platform a)-magnification 13kX, b)-magnification 40kX and inset 300kX, c) TEM image of CNW@Au on the edges and d) on the inner walls

The gold nanoparticles anchored on the edges and also onto the inner walls of CNW, can create “super lenses” as resonant amplifiers and nano-concentrators [30], of the incident radiation. Fig. 5 shows the SERS signals of the Rhodamine B loaded on carbon nanowalls decorated with gold nanoparticles (i.e. on Au@CNW platforms), at several Rhodamine concentrations from  $10^{-4}$ ,  $10^{-8}$  and  $10^{-10}$  M. The assignment of bands [11,31-33] appearing in Fig. 5 is presented in Table 1 on various supports (Ag@CNW, Ag/ZnO, Ag on paper substrates and Au@SiO<sub>2</sub>@Ag).

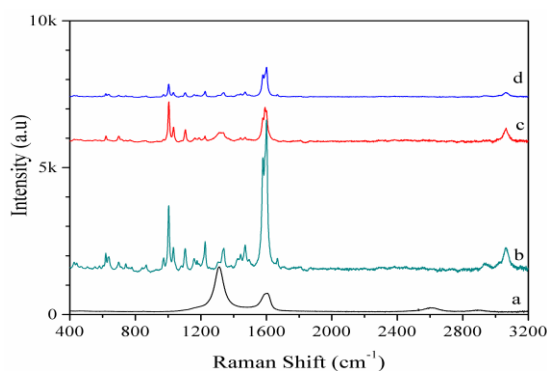


Fig. 5. The Raman spectra of different concentrations of Rhodamine B ( a-0 M, b- $10^{-4}$  M, c)- $10^{-8}$  M and d- $10^{-10}$  M) on hybrid platform (Au@CNW)

We observed the bands near  $738\text{cm}^{-1}$  corresponding to  $\text{C}_x\text{-H}$  out of plane bend, bands at about  $620\text{ cm}^{-1}$  due to  $\text{C}_x\text{-C}_x\text{-C}_x$  ring-bend and bands corresponding to aromatic stretching vibrations at  $1000$ ,  $1102$ ,  $1224$ ,  $1466$ ,  $1575$ ,  $1600$  and  $1662\text{ cm}^{-1}$ , corresponding to  $\text{C}_x\text{-H}$ ,  $\text{C}_x\text{-O-C}_x$ ,  $\text{C}_E\text{-H bend} + \text{CC}_x\text{-H}$ , and  $\text{C}_x\text{-C}_x$  (see Table 1).

Table 1. Assignment of peaks from the Raman SERS spectra of Rhodamine B

Peak positions from literature and present work, Raman Shift of RhB [ $\text{cm}^{-1}$ ]					Assignment
[11]	[31]	[32]	[33]	Present work	
608	620	613	622	620	$\text{C}_x\text{-C}_x\text{-C}_x$ bend
770	763		732	738	$\text{C}_x\text{-H}$ out of plane bend
	931		931	968	$\text{C}_x\text{-C}_x\text{-C}_x$ bend
	1075		1075	1000, 1033	$\text{C}_M\text{-H}$ bend
1122			1123	1102	$\text{C}_x\text{-H}$ in plane bend
1182		1195	1192	1158	$\text{C}_x\text{-C}_x$ bend str
	1191				
		1278	1278	1224	$\text{C}_x\text{-O-C}_x$ str
	1277				
1302	1355			1335	$\text{C}_x\text{-C}_x$ bend str
1360		1355	1355		C-N bend str
				1466	$\text{C}_E\text{-H bend} + \text{CC}_x\text{-H}$
1505	1504	1504	1503		
	1526	1525			
1582	1560		1580	1575	$\text{C}_x\text{-C}_x$ bend str
	1594		1603	1600	$\text{C}_x\text{-C}_x$ bend str
1651	1644	1644	1642	1664	$\text{C}_x\text{-C}_x$ bend str

We note also a red shift for the Raman band assigned to aromatic stretching (exception making the peak at  $1662\text{ cm}^{-1}$ ), which can be caused by the substrate roughness and the adsorption of benzene rings on the nanowalls surfaces. For quantitative analysis, we selected the Raman line at  $1000\text{ cm}^{-1}$ , because it can be found in all of the spectra and it is strongly dependent on the Rhodamine B concentration. The dependence of this line intensity upon the Rhodamine B concentration in solution is shown in Fig. 6. According to Fig. 6, the Raman intensity decreases gradually with the decrease in concentration from around 2400 a.u. at  $10^{-4}\text{ M}$  to 500 in the case of  $10^{-10}\text{ M}$ . Still, a measurable signal was obtained at the lowest concentration. The carbon nanowalls decorated with gold nanoparticles exhibit a high enhancement factor,  $2,5 \times 10^9$ . This value was calculated according to the procedure of Wang and co-workers [34,35]. The improvement comes from using smaller nanoparticles size and density [36], using gold as material and, possibly, from the larger specific area of the CNW support that can be increase by variation of deposition parameters [37].

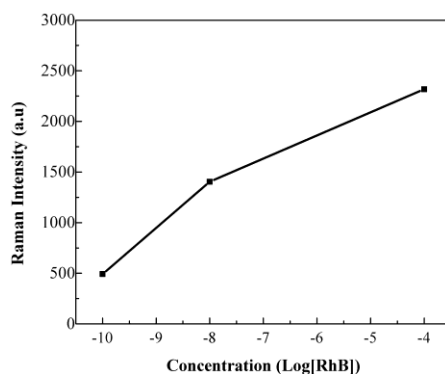


Fig. 6. The relationship between the Raman intensity at  $1000\text{ cm}^{-1}$  and the Rhodamine B concentrations

#### 4. Conclusions

We have developed 3D platforms for Surface-Enhanced Raman Spectroscopy with increased sensitivity compared to those based on uncoated carbon nanowalls or gold nanoparticles on flat surfaces. The platform for loading the analytes was obtained by uniform decoration of carbon nanowalls with gold nanoparticles using a chemical method. The as-obtained Au@CNW supports are efficient SERS substrates for detecting Rhodamine B in solution with concentrations as low as  $10^{-10}$  M. The observed Raman enhancement is related to the high affinity of Rhodamine B for the aromatic rings on the graphene domains of CNW, to the large number of gold nanoparticles dispersed on the high surface area offered by the open architecture of the CNW layers, and to the effective focusing of the light by the synthesized gold nanoparticles. These results are relevant for development of optical sensing platforms based on the SERS effect.

#### Acknowledgments

This work was supported by a grant of the Romanian Ministry of Research and Innovation, CCCDI - UEFISCDI, project number PN-III-P1-1.2-PCCDI-2017-0172/ PCCDI-15/2018-TESTES, within PNCDI III.

#### References

- [1] C. David, N. Guillot, H. Shen, T. Toury, M. L. de la Chapelle, *Nanotechnology* **21**, 475501 (2010).
- [2] M. Green, F. M. Liu, L. Cohen, P. Köllensperger, T. Cass, *Faraday Discussions*. **132**, 269 (2006) .
- [3] R. A. Karaballi, A. Nel, S. Krishnan, J. Blackburn, C. L. Brosseau, *Phys. Chem. Chem. Phys.* **17**, 1356 (2015).
- [4] P. Kao, N. A. Malvadkar, M. Cetinkaya, H. Wang, D. L. Allara, M. C. Demirel, *Adv. Mater.* **20**, 3562 (2008).
- [5] H. Liu, L. Zhang, X. Lang, Y. Yamaguchi, H. Iwasaki, Y. Inouye, Q. Xue, M. Chen, *Sci. Rep.* (2011) doi:10.1038/srep00112.
- [6] J. A. Dieringer, R. B. Lettan II, K. A. Scheidt, R. P. Van Duyne, *J. Am. Chem. Soc.* **129**, 16249 (2007).
- [7] S. Nie, S. R. Emory, *Science* **275**, 1102 (1997).
- [8] E. C. Le Ru, M. Meyer, P. G. Etchegoin, *J. Phys. Chem. B* **110**, 1944 (2006).
- [9] K. Kneipp, Y. Wang, H. Kneipp, L. T. Perelman, I. Itzkan, R. R. Dasari, M. S. Feld, *Phys. Rev. Lett.* **78**, 1667 (1997).
- [10] A. N. Grigorenko, M. Polini, K. S. Novoselov, *Nat. Photonics* **6**, 749 (2012).
- [11] C. S. Rout, A. Kumar, T. S. Fisher, *Nanotechnology* **22**, 395704 (2011).
- [12] Y. Zhao, G. Chen, Y. Du, J. Xu, S. Wu, Y. Qu, Y. Zhu, *Nanoscale* **6**, 13754 (2014).
- [13] H. Zhao, H. Fu, T. Zhao, L. Wang, T. Tan, *J. Colloid. Interface. Sci.* **375**, 30 (2012).
- [14] Y. Tan, Y. Gu, L. Xu, X. Zhang, D. Liu, W. Zhang, Q. Liu, S. Zhu, H. Su, C. Feng, G. Fan, D. Zhang, *Adv. Funct. Mater.* **22**, 1578 (2012)
- [15] M. E. Stewart, C. F. Anderton, L. B. Thompson, J. Maria, S. Gray, J. Rogers, R. Nuzzo, *Chem. Rev.* **108**, 494 (2008).
- [16] H. Ko, S. Singamaneni, V. V. Tsukruk, *Small* **4**, 1576 (2008).
- [17] S. Siddhanta, V. Thakur, C. Narayana, S. M. Shivaprasad, *ACS Appl Mater Interfaces* **4**, 5807 (2012).
- [18] X. Ling, L. Xie, Y. Fang, H. Xu, H. Zhang, J. Kong, M. S Dresselhaus, J. Zhang, Z. Liu, *Nano Letters* **10**, 553 (2009).
- [19] L. Wu, H. S. Chu, W. S. Koh, E. P. Li, *Optics Express* **18**, 14395 (2010).
- [20] J. Parisi, L. Su, Y. Lei, *Lab Chip* **13**, 1501 (2013).
- [21] J. Prinz, A. Matkovic, J. Pesic, R. Gajic, I. Bald, *Small* **12**, 5458 (2016).

- [22] A. E. Rider, S. Kumar, S. A. Furman, K. Ostrikov, *Chem Commun.* **48**, 2659 (2012).
- [23] R. Ion, S. Vizireanu, C. E. Stancu, C. Luculescu, A. Cimpean, G. Dinescu, *Mater. Sci. Eng. C-Mater. Biol. Appl.* **48**, 118 (2015).
- [24] S. Vizireanu, B. Mitu, C. R. Luculescu, L. C. Nistor, G. Dinescu, *Surf. Coat. Technol.* **211**, 2 (2012).
- [25] A. Felten, C. Bittencourt, J. F. Colomer, G. Van Tendeloo, J. Pireaux, *Carbon* **45**, 110 (2007).
- [26] S. Mihai, *Acta. Phys. Pol. A* **123**, 254 (2013).
- [27] S. Mihai, A. Dinescu, L. C. Nistor, D. Ciuparu, *Adv. Sci. Eng. Med.* **6**, 399 (2014).
- [28] D. J. Cott, M. Verheijen, O. Richard, I. Radu, S. D. Gendt, S. V. Elshocht, P. M. Vereecken, *Carbon* **58**, 59 (2013).
- [29] S. Vizireanu, A. Lazea Stoyanova, M. Filipescu, D.L. Cursaru, G. Dinescu, *Dig. J. Nanomater. Biostruct.* **8**, 1145 (2013).
- [30] S. V. Boriskina, B. M. Reinhard, *Proc. Natl. Acad. Sci.* **108**, 3147 (2011).
- [31] C. H. Sun, M. L. Wang, Q. Feng, W. Liu, C. X. Xu, *Russian. J. Physic. Chem. A* **89**, 291 (2015).
- [32] S. Lin, W. L. J. Hasi, X. Lin, S. Han, X. T. L. Lou, L. F. Yang, D. Y. Lin, Z. W. Lu, *Anal. Methods* **7**, 5289 (2015).
- [33] D. Li, D. W. Li, J. S. Fossey, Y. T. Long, *J. Mater. Chem.* **20**, 3688 (2010).
- [34] R. Wang, Y. Xu, R. Wang, C. Wang, H. Zhao, X. Zheng, X. Liao, L. Cheng, *Microchimica Acta* **184**, 279 (2017)
- [35] R. Wang, Y. Xu, C. Wang, H. Zhao, R. Wang, X. Liao, L. Chen, G. Chen, *Appl. Surf. Sci.* **349**, 805 (2015)
- [36] A. McLeod, S. Kumar, K. C. Vernon, K. Ostrikov, *J. Nanomater.* 230987 (2015)
- [37] S. Vizireanu, M. D. Ionita, R. E. Ionita, S. D. Stoica, C. M. Teodorescu, M. A. Husanu, N. G. Apostol, M. Baibarac, D. Panaitescu, G. Dinescu, *Plasma Process. Polym.* (2017), doi: 10.1002/ppap.201700023.